*2010 3rd International Conference on Computer and Electrical Engineering (ICCEE 2010)*
***IPCSIT vol. 53 (2012) © (2012) IACSIT Press, Singapore***
*DOI: 10.7763/IPCSIT.2012.V53.No.2.41*

# Dependence of IGBT Junction-Case Steady State Thermal Resistance on Heating Current

Ming Chen+, Yong Tang and Bo Wang

National Key Laboratory for Vessel Integrated Power System Technology, Naval University of Engineering

Wuhan, 430033, China

**Abstract—** High heating current dependence of the IGBT module junction-case steady state thermal resistance is investigated. The conception of the thermal resistance and the physical structure of the IGBT module and the thermal impedance test principle are briefly introduced. The junction-case thermal resistance can be deduced by Finite Element Method in the numerical simulator ANSYS. The transient thermal impedance curve and the junction-case steady state thermal resistance of a certain type of IGBT are obtained by the thermal resistance test experiments. It's found that the junction-case steady state thermal resistance decreased when the heating current increased. When the high heating current reaches a certain level, the steady state thermal resistance becomes a constant.

**Keywords**- IGBT, thermal resistance, junction temperature, heating current, transient thermal impedance, case temperature

## 1. Introduction

THE operating junction temperature of the IGBT module is an important factor affecting both operating performance and service lifetime [1]-[2]. One method for calculating the junction temperature is to find the thermal impedance of the module and determine the temperature rise above case temperature by multiplying the thermal impedance by the power dissipated in the module [3]. A common error is to assume that the junction-case steady state thermal resistance is a constant under any test condition. However, the junction-case steady state thermal impedance of the heterojunction bipolar transistors (HBT) is not constant but a function of both the power dissipation and the ambient temperature [3]-[6].

The junction-case steady state thermal resistance is one of the most important parameters given in an IGBT datasheet, but it is often specified ambiguously, resulting in a value which is of not much practical use to the devices user [2]. The majority of manufacturers' datasheets give values for the junction-case steady state thermal resistance without specifying either the measurement technique used or related test conditions. The junction-case steady state thermal resistance values vary by a factor of two or more depending on these associated parameters [2], if the unwary designer uses a value of the thermal resistance without knowing under what conditions it was measured, both the performance and the reliability of the final design may suffer. This paper attempts to clarify the thermal resistance test principle and condition, especially under different high heating current, and simulation verification with the Finite Element Method in the numerical simulator ANSYS is also included.

In this paper, the IGBT multilayer physical structure and conception of thermal resistance are presented in Section II. In order to obtain the thermal resistance, Section III presents the principle of extract the transient thermal impedance curve. Section IV discusses the changes of the physical and electrical parameters that due

+ Corresponding author.
*E-mail address*: chmwhhb99@163.com

to the different heating current. In Section V, the Finite Element Method in the numerical simulator ANSYS is used as simulation tool, also the simulation results and its' discussion are shown. Section VI presents the experimental results and its' analysis.

## 2. Theoretical Background: The Evaluation of The Thermal Transient Measurements

The dynamic thermal property of the IGBT package is usually measured by the thermal resistance. In the $t = 0$ time instant a $P_{diss}$ dissipation-step is applied to the package. Beginning with this moment the $\Delta T(t)$ temperature rise of the die is continuously recorded. This function is called the heating curve. This curve is called the transient thermal impedance curve [7]. The junction-case thermal resistance can be expressed as follow

$$R_{thJC} = \frac{T_J - T_C}{P_{diss}} \tag{1}$$

where $T_J$ is the junction temperature, $T_C$ is the case temperature, $P_{diss}$ is the dissipated power, and $R_{thJC}$ is the equivalent junction-case steady state thermal resistance.

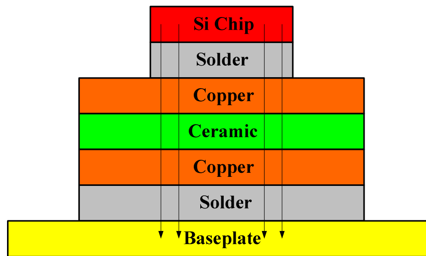


Fig.1 Structure of the IGBT Module

The multilayer physical structure of the IGBT module is shown in Fig.1. It's usually consists of 7 layers [7]. As for each layer of the IGBT module, the area is greatly larger than the thickness. Thus for simplification, the IGBT module can be seen as one-dimensional structure. The heat that flows into the first surface has to flow out through the second. Ignoring the lateral heat dissipation and convection and thermal radiation, all the heat is transfer in vertical direction [1].

## 3. Extraction of Thermal Resistance

In this part, the method to extract the thermal resistance is briefly studied [9].

### 3.1. Method to detect junction temperature

From equation (1), the method to detect junction temperature is of essential importance. Infrared microscopy and the Thermal Sensitive Electrical Parameter (TSEP) are prevalent methods to detect junction temperature [10]. For infrared microscopy can only fits for detect the unpackaged devices, thus, in order to detect junction temperature of IGBT, the package should be unsealed. Such method effects the precise of the test results. TSEP measurement technique provides a quick, nondestructive determination of die-to-case attachment quality. Compare with infrared microscopy, the TSEP possess quick-detecting, more precise, low experimental cost. The TSEP method does not require coating the Device Under Test (DUT) with any sort of material [2].

### 3.2. Extract the junction temperature calibration curve

The junction temperature is determined using the almost linear temperature dependent voltage across the collector-emitter $V_{CE}$ while in forward condition.

The thermal resistance test is composed of two steps, the first step is: determination of the temperature coefficient of the collector-emitter voltage at the low measuring current.

The diagram of extracting the temperature coefficient is shown in Fig.2. A current source supplies a low continuous direct sampling collector current $i$ which is just sufficient to raise the collector-emitter voltage $V_{CE}$ above the saturation value. $S1$ is the DUT. The collector-emitter voltage drop is measured at different ambient

temperature, which equals to the junction temperature, for $S1$ is put into a constant temperature oven. Then the relationship between $V_{CE}$ and $T_J$ can be got by curve fitting.

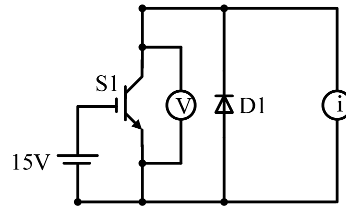


Fig.2 Circuit of extract the temperature coefficient

### 3.3. Thermal resistance test

The second step of the thermal resistance test is: measurement of the response of the IGBT to a step change in the internal power dissipation.

Thermal resistance test circuit is shown in Fig.3. $I$ is a high collector current for heating up $S1$. The low sample current $i$ is always on. The high heat current $I$ is on for a certain amount of decided time. Then it is turned off, the measure equipments measure the essential data every sample time.

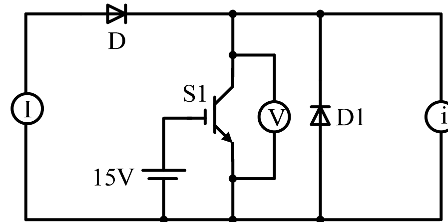


Fig.3 Thermal resistance test circuit

## 4. Theoretical Qualitative Analysis

This part describes different heating current effect the electrical and thermal parameters.

### 4.1. Distribution of high heating current on the chip surface

The junction temperature varies from point to point along the surface of the die [2]. When the high heating current becomes increased, the current distribution becomes more asymmetric, which leads to that the junction temperature changes greatly from point to point on the die surface. The temperature dependent electrical model is based upon temperature dependent IGBT model parameters and the temperature dependent physical properties of each layer material [8].

### 4.2. self-heating effect

As the junction temperature rise, the case temperature also rises at the same time, with the self-heating effect [5], the temperature of each layer rises at the same time.

### 4.3. Variation of material thermal conductivity [11-12] and volumetric heat capacity values [13]

It is well-known that the thermal conductivity changes with temperature [11]-[13]. For many of the materials used in the IGBT modules the thermal conductivity $\lambda(T)$ as function of temperature $T$ is approximately as

$$\lambda(T) = \lambda_{ref}\left(\frac{T}{T_{ref}}\right)^{-\alpha} \tag{2}$$

in the relevant temperature range. Here $\lambda_{ref}$ is the thermal conductivity at the reference temperature $T_{ref}$. For Si one often sees $\alpha = 4/3$ being used. More specific, equation (2) becomes

$$\lambda(T) = 154.86\left(\frac{T}{300}\right)^{-\frac{4}{3}} \tag{3}$$

Ref. [14-15] uses Kichhoff transformation to deal with temperature dependent physical properties of each layer material.

### 4.4. Different voltage drop

Table II shows the collector-emitter voltage drop at different heating current.

TABLE II: VOLTAGE DROP AT DIFFERENT HEATING CURRENT

| Heating current/A | Voltage drop/V |
| --- | --- |
| 30 | 1.51 |
| 40 | 1.70 |
| 50 | 1.90 |
| 60 | 2.11 |
| 70 | 2.35 |
| 80 | 2.64 |
| 90 | 3.01 |

As Table II shows, the high heating current rises, the collector-emitter voltage drop increases, thus the dissipated power increases.

## 5. Simulation Verification and Discussion

### 5.1. 3-D thermal modeling

Thermal numerical analysis is performed with a commercially software ANSYS using finite element method [10]. The final structured mesh has 50177 elements and 192256 nodes. Inside the IGBT module, the dominant heat transfer mechanism is thermal conduction between different layers, convection and radiation of the different materials to ambient is ignored. The base-plate temperature is set to 50℃, operating current is 80A, the collector-emitter voltage drop is 2.61V.

### 5.2. Simulation results and discussion

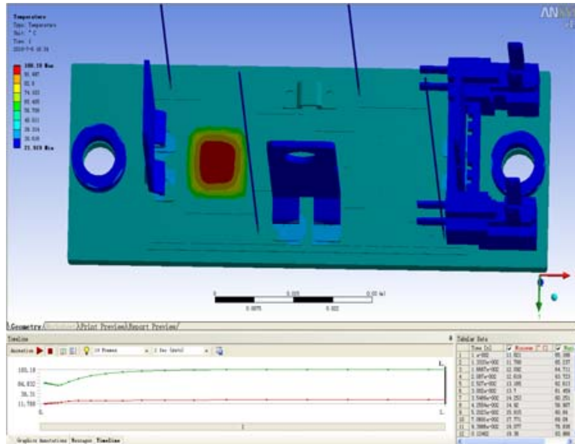

Fig.4 Simulation diagram of temperature field distribution

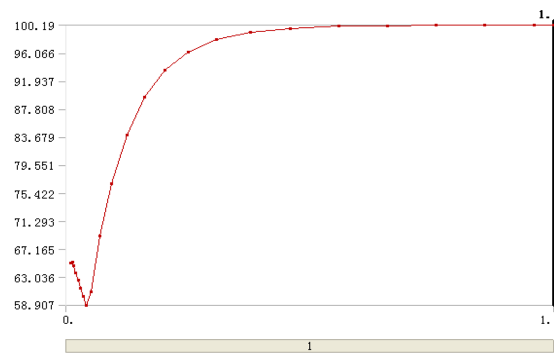


Fig.5 Simulation rise curve of peak junction temperature

Simulation results of temperature field distribution is shown in Fig.4. Simulation rise curve of peak junction temperature is shown in Fig.5. In Fig.5, the abscissa represents the time, the unit is second. the y-axis represents the temperature, the unit is ℃.

From Fig.5, the steady state peak junction temperature equals to 100.2℃, then the junction-case thermal resistance is

$$R_{thJC} = \frac{100.2 - 50}{80 \times 2.64} = 0.237 \tag{4}$$

TABLE III shows the simulation results of steady-state junction-case thermal resistance at different high heating current.

TABLE III: THE THERMAL RESISTANCE AT DIFFERENT HIGH HEAT CURRENT

| High heating current/A | Thermal resistance ℃/W |
|---|---|
| 30 | 0.15 |
| 40 | 0.18 |
| 50 | 0.20 |
| 60 | 0.22 |
| 70 | 0.23 |
| 80 | 0.24 |
| 90 | 0.25 |

Compare with the method the average temperature of the die surface chosen as the junction temperature, the simulation results are larger, for the peak temperature of the die surface chosen as the junction temperature.

## 6. Experimental Results

The platform for extract the IGBT transient thermal impedance curve is shown in Fig.6. All the measure equipments are controlled by LabVIEW 8.5.

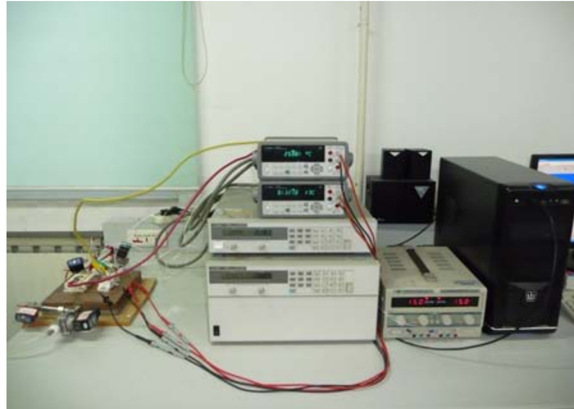

Fig.6 Platform for IGBT thermal resistance test

Fig.7 shows a GD50HFL120C1S module for the thermal resistance test. The case temperature is measured by a thermocouple. TSEP uses the average temperature of the die surface as the junction temperature.

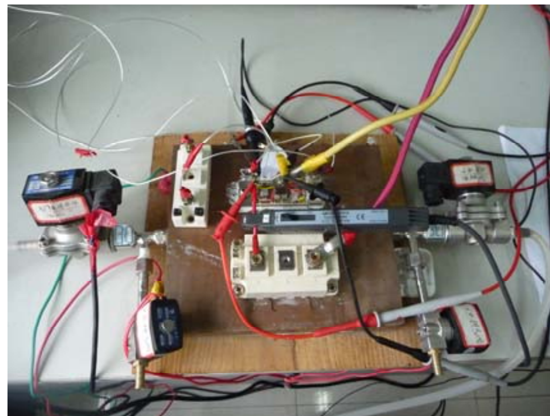

Fig.7 The IGBT module for thermal resistance test

The sample current $i$ equals to 0.1A in this paper. A DUT is put into a constant temperature oven, and is heated up from 40℃ to 150℃.

The measured results are shown in Fig.8.

Based upon the measured data, with the method of least square cure fitting, the calibration curve between the junction temperature $T_J$ and the voltage drop $V_{CE}$ can be derived as follow

$$T_J = 281 - 453V_{CE} \quad (5)$$

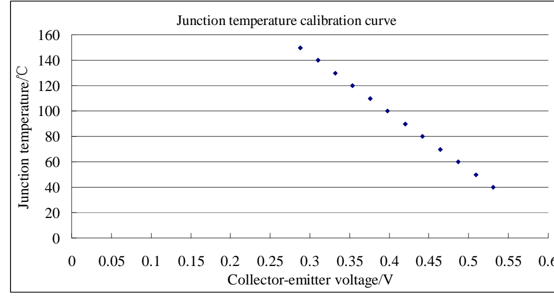


Fig.8 The junction temperature calibration curve

The high heating current $I$ equals to 90A, and sample once every 10s. The transient thermal impedance curve can be seen as Fig.9 shown. $R_{thJC}$ equals to 0.22℃/W.

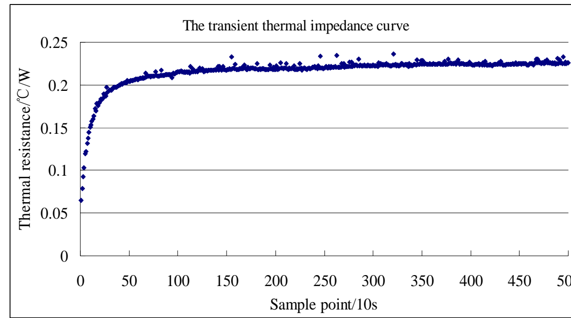


Fig.9 The transient thermal impedance curve

The heat sink condition as Fig.7 shows, the DUT is put on the cool-plate, and the water is flows in the pipe. Such suitable heat-sink can keep the case temperature nearly constant. The thermal resistance test results at different high heating current are shown in table IV.

TABLE IV: THE THERMAL RESISTANCE AT DIFFERENT HIGH HEAT CURRENT

| Heating current/A | Thermal resistance ℃/W |
|---|---|
| 30 | 0.16 |
| 40 | 0.17 |
| 50 | 0.18 |
| 60 | 0.19 |
| 70 | 0.20 |
| 80 | 0.21 |
| 90 | 0.22 |

From TABLE IV, it can clearly be seen that the value of $R_{thJC}$ related to the high heat current. It is increased when the heating current increases.

## 7. Conclusion

The high heating current dependence of the IGBT junction-case steady state thermal resistance is investigated. It is found that the junction-case steady state thermal resistance is related to the heat current. It is increased when the heating current increases. When the high heating current $I$ reaches a certain level, the steady state thermal resistance becomes a constant.

## 8. Acknowledgment

This research is subsidized by National Natural Science Foundation of China (NSFC) for the Key Award Project (50737004) and the National Natural Science Foundation of China (NSFC) for Innovation Research Group under Grant 50721063.

## 9. References

[1] Masana F N, “A new approach to dynamic thermal modelling of semiconductor packages,” Micro-electronics Reliability, 2001, 41, pp. 901-912.
[2] Hewlett-Packard, “A guide to understanding, measuring, and applying power FET thermal resistance coefficients,” High-frequency transistor primer part III-A: thermal resistance.
[3] S P Marsh, “Direct extraction technique to derive the junction temperature of HBT’s under high self-heating bias conditions,” IEEE T-Electron Devices, Vol. 47, No. 2, pp. 288-291, February 2000.
[4] N Bovolon, P Baureis, J E Muller, et al. “A simple method for the thermal resistance measurement of AlGaAs/GaAs Heterojunction Bipolar Transistors,” IEEE T-ED, Vol. 45, No. 8, pp. 288-291, August 1998.
[5] N Rinaldi, “Small-signal operation of semiconductor devices including self-heating, with application to thermal characterization and instability analysis,” IEEE T-ED, Vol. 48, No. 2, pp. 323-331, February 2001.
[6] J C J Paasschens, S Harmsma, R Toorn, “Dependence of thermal resistance on ambient and actual temperature,” IEEE BCTM 5.1.
[7] U drofenik, J W Kolar, “Teaching thermal design of power electronic systems with web-based interactive educational software,” IEEE APEC 2003, Miami, Florida, USA, 18, pp. 1029-1036.
[8] J Reichl, D Berning, A Hefner, J Lai, “Six Pack IGBT Dynamic Electro-Thermal Model: Parameter Extraction and Validation,” IEEE APEC’04, Anaheim, CA, 2004, pp. 246-251.
[9] Rthjc - IEC 60747-9 Ed2/CD.
[10] D L Blackburn, “Temperature measurements of semiconductors devices – a review,” 20th SEMI- THERM Symposium, Gaitherburg, 2004.
[11] F F Oettinger, D L Blackburn, S Rubin, “Thermal characterization of power transistors,” IEEE Transaction on Electron Devices, Vol. 23, No. 8, pp. 831-838, August 1976.
[12] D L Blackburn, F F Oettinger, “Transient Thermal Response Measurements,” IEEE Transaction on Industrial Electronics and Control Instrumention, Vol. 22, No. 2, pp. 134-141, May 1975.
[13] M Rencz V Szekely, “Non-linearity issues in the dynamic compact model generation,” 19th IEEE SEMI-THERM Symposium, pp. 263-270.
[14] V R Voller, “Numerical treatment of rapidly changing and discontinuous conductivities,” International journal of heat and mass transfer, 2001, vol. 44, pp. 4553-4556.
[15] F Bonani, G Ghione, “On the application of the Kirchhoff transformation to the steady-state thermal analysis of semiconductor devices with temperature- dependent and piecewise inhomogeneous thermal conductivity,” Solid-State Electronics, Vol. 38, No.7, pp.1409-1412, 1995.